SSRG International Journal of Electrical and Electronics Engineering
ISSN: 2348-8379 / https://doi.org/10.14445/23488379/IJEEE- V10I2P106

Volume 10 Issue 2, 61-74, February 2023

Original Article

Thinning Approach based on Sides Lobe Level Reduction in the Linear Array Antenna using Dynamic Differential Evolution

Anitha Suresh[1], C. Puttamadappa[2], Manoj Kumar Singh[3]

[1,2]*Department of Electronics and Communication, Dayananda Sagar University, Bangalore, India*
[3]*Manuro Tech Research Pvt. Ltd., Bangalore, India*

[1]*Corresponding author: anisuri2011@gmail.com*

Received: 08 January 2023 Revised: 06 February 2023 Accepted: 16 February 2023 Published: 28 February 2023

Abstract *- This novel work has considered the problem of minimizing the side lobe level of linear array antenna patterns using the concept of thinning. In comparison to all element arrays, thinning approach activated only a fraction portion of the total available number of array elements at the suitable positions to achieve the objectives. The thinning problem has been transformed into a constrained optimization problem with the objective of minimizing the total number of activated array elements while simultaneously satisfying the desired side lobe and first null beam width. A new approach based on dynamic value assignment of mutation factor in the differential evolution has been proposed, which carries the random value assignment for each component of the differential vector. The proposed dynamic mutation factor assignment helped to explore and converge on a better solution compared to the standard approach. Fundamentally Differential evolution explores the solution over a continuous domain; hence a transformation is needed to convert the solution into the binary domain for thinning. The different existing forms of transformation, including sigmoid function-based S-shaped and V-shaped functions, have been considered under probabilistic and threshold-based binary conversion processes. It has been observed that the proposed form of differential evolution has explored a better solution by rounding the obtained real value to the nearest integer value and later assigning the binary value according to closeness to their binary value limit. For the linear array detail, experimental analysis has given and observed that the proposed solution has outperformed not only other variants of differential evolution but also performed better than particle swarm optimization results available in past literature.*

Keywords *- Array antenna, Thinning, Side lobe level, Linear array, Differential evolution.*

1. Introduction

Antenna arrays are critical in detecting and processing information coming from various directions. Antenna array synthesis aims to achieve a physical architecture of the array with a radiation pattern near the required pattern. An antenna array is made up of many fixed antenna units that are often supplied coherently. Various antenna array applications have recently been proposed to improve the performance of mobile and wireless communication systems, such as effective spectrum usage, expanding channel capacity, extending coverage area, modifying beam shape, and so on. One of the most common antenna array difficulties is constructing a set of feeding values that must be applied to an array's ports to generate a radiation pattern that meets certain parameters. This is commonly referred to as synthesis. The fundamental goal of antenna research is to enhance array patterns by altering structural geometry to decrease SLL while keeping the main beam gain. In such antenna array geometry synthesis procedures, the objective is to discover the physical structure of the array that provides the radiation pattern closest to the intended pattern. Many synthesis approaches coexist because the form of the intended pattern might vary greatly depending on the application.

Array thinning is a major method of synthesis that we hope would not only lower the side lobe level (SLL) but also reduce the number of array components and, therefore, significantly reduce cost. Array thinning is also a good way to make a compromise between low SLL and narrow beams. Low-side lobes offer mediocre defense against interfering signals that are incident on the array from any angle other than the main beam. Additionally, since random errors raise the side lobe level, lowering the side lobe level necessitates tighter tolerances on array components. A uniformly spaced or periodic array can be thinned by turning off some of its elements to achieve the desired amplitude density across the aperture. A component linked to the feed network is "on," whereas a component linked to a matched load is "off".. Thinning approaches can be applied to linear as well as planer arrays.

The problem of optimizing the array pattern with respect to the element locations becomes complex and nonlinear because the array factor of the thinned array is a nonlinear function of element spacing, and there are an infinite number of combinations of element locations. Some detailed methods like the Perturbation technique, linear programming, dynamic programming and the Mini–Max [1–5]. Recently, approaches like Genetic Algorithms [1], Particle swarm Optimization [2,3], Invasive weed optimization [4] and differential evolution [5] achieved success in designing antenna arrays which have difficult array geometry. In [6,7,18], a stochastic algorithm-like synthesis of thinned concentric ring arrays is presented. However, designing thinned antenna arrays with numerous radiating elements is a challenging task. It requires the use of effective numerical techniques to solve complex, nonlinear, and non-differentiable functions. [32] Had mentioned three techniques to upgrade the performance of an array aperture by interleaving arrays within the same aperture vicinity. With a uniform spacing of interleaved arrays that are integer multiples of minimum set spacing and are enhanced to lessen the highest side lobe level. The technique of interleaving elements of multiple arrays uses aperture area effectively. [9] Had verified that it is possible to interleave a thinned sum array with a thinned distinction array to use an existing aperture effectively. Non-uniform antenna array synthesis with as few elements as possible has appreciable practical applications. [10] It has introduced a new non-iterative approach for linear array synthesis, which relies on the matrix pencil method (MPM).

The latest method towards compact integration, discussing the initial design of a Ku-band, metallic-waveguide fed active/passive array leading to a more price-effective technology for array feeds, has been discussed in [12]. In [13] combination of the method of moments (MoM) and the genetic algorithm (GA) based hybrid technique for synthesizing arbitrary-shaped radiation patterns with a linear array is presented. In [14] Thinning of CCA using FFA has been presented. Bayesian inference framework [15] has focused on the various sensible design issues, like the demand for less spacing between two adjacent array elements, restrictions in the dynamic range and correctness of the current amplitudes and phases, the ability to generate multiple required radiation patterns using a single array and the capacity to maintain a required radiation pattern over a certain frequency band. [16] Has discussed the issue of interference suppression by minimizing the side lobe. Synthesis of linear antenna array by the usage of Continuous Genetic Algorithm is achieved to search for the top-quality amplitude weights to decrease the most side lobe stage. A broadband, twin polarization, and absolutely narrow beam (<11°) antenna array gadget primarily based on the Long Slot Antenna (LSA) array technology has been proposed in [17] for wireless communication. The complicated feeding structure of the antenna array becomes simplified with an aperture metal patch design using 50 - 60Ω micro-strip lines. Direction-of-arrival (DOA) of radio indicators takes a splendid technological interest in radar, sonar and wi-fi communication tasks. The problem of DOA estimation methods for circular and concentric circular antenna arrays is being discussed in [23,33]. The paper [19] has presented an approach concerning designing non-uniform linear antenna arrays with symmetrical factors and using multi-criteria optimization with genetic algorithms. The intention was to improve the radiation pattern to get it toward the favored one, using non-uniform distances between elements and a non-uniform distribution of currents thru the factors for attaining higher efficiency. The usage of ecology-based Flower Pollination Algorithms (FPA) on the antenna array over linear antenna array is discussed in [20].

A differential evolution-based approach has been applied to obtain the linear array antenna's thinning. The exploration quality of differential evolution has increased by providing an independent mutation factor to each element of the differential vector. The different transformation strategies have been applied to change the explored continuous solution to a binary solution. To satisfy the constraint of the desired value of SLL and FNBW, a penalty-based strategy has been used to make the solution feasible. The paper has been divided into a number of sections to share information compactly. Section 2 carried the detailed mathematical model of the problem. The proposed solution has been discussed in detail in section 3, while extensive experimental results and discussion have been given in section 4. The conclusion has given at the end in section 5.

2. Modeling of Linear Array Antenna

2.1. Linear Array Antenna

Let us assume we have 2N isotropic radiators arranged along the x-axis symmetrically, as shown in Figure 1, so we can design a linear antenna array.

Equation 1 can be used to determine the far-field array factor for the 2N isotropic elements.

$$AF(\theta) = 2\sum_{n=1}^{N} I_n Cos\left[\frac{2\pi}{\lambda} x_n cos(\theta) + \varphi_n\right] \quad (1)$$

Where I_n denotes the excitation magnitude, φ_n the excitation phase and θ the angle from the array line.

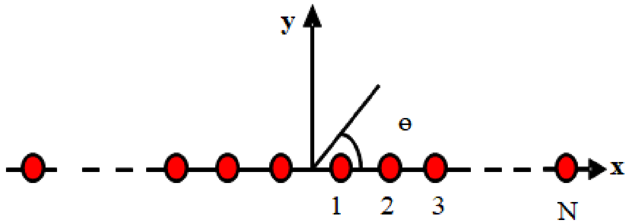

Fig. 1 2N elements in a linear array on the x-axis

The nth element is located at x_n. Additional presumptions regarding the uniform excitation of I_n amplitude and phase φ_n as 0 for all elements have been made.

2.2. Design Considerations

For a specified PSLL and FNBW, thinning of the linear array has to be done to achieve the desired objectives with a minimum number of array elements. The assumption has been made that all elements have the same excitation and a phase of 0°. Thinning has represented by considering the 'on' element as '1' while the 'off' element as '0', as shown in Eq.4.

$$I_{mn} = \begin{cases} 1 & if\ \ m^{th}\ ring, n^{th}\ element\ \ is\ 'on' \\ 0 & if\ \ m^{th}\ ring, n^{th}\ element\ \ is\ 'off' \end{cases} \quad (2)$$

The design has been considered in the X-Z plane ($\phi = 0^o$) and the main beam has achieved its maximum in the direction of $\theta_0 = \phi_0 = 0^0$.

2.3. Objective Function

f : *minimize* {Total number of array elements}

Subjected to constraints

$$\begin{cases} PSLL_{obtained} \leq PSLL_{desired} \\ FNBW_{obtained} \leq BW_{desired} \end{cases} \quad (3)$$

The objective function f defined in Eq.3, which has to minimize to achieve the minimum number of array elements (NAE) while satisfying the constraint of desired PSLL and FNBW, can be represented in mathematical form as given in Eq.4

$$F = K_1(|PSLL_d| - |PSLL_o|)H(T1) + K_2(FNBW_d - FNBW_o)H(T2) + NAE \quad (4)$$

Where, $K_1\, and\, K_2$ are the penalties constant, and should they be considered large values like 1000 or more. $T1\ and\ T2$ are the parameter of the Heaviside step function and have the values given by Eq.5

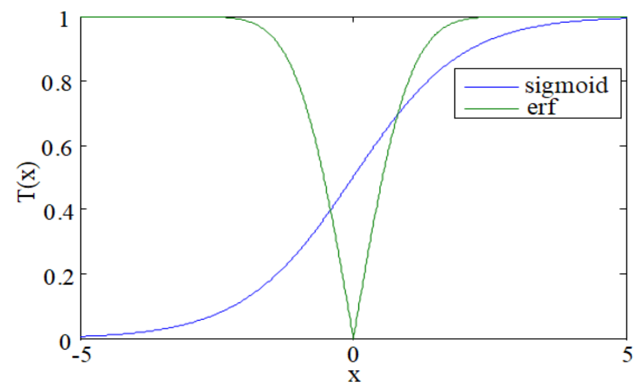

Fig. 2 Graph of S-shape and V-shaped transfer function

$$\begin{aligned} \mathrm{T1} &= (|\mathrm{PSLL_d}| - |\mathrm{PSLL_o}|) \\ \mathrm{T2} &= (\mathrm{FNBW_d} - \mathrm{FNBW_o}) \end{aligned} \quad (5)$$

The Heaviside step function $H(T)$ defined by Eq.6

$$H(T) = \begin{cases} 0 & if\ \ T \leq 0 \\ 1 & if\ \ T > 0 \end{cases} \quad (6)$$

3. Proposed Solution

The novelty in the thinning approach of array antenna has been fulfilled in this work over two different perspectives: (i) designing a better continuous meta-heuristics over the platform of differential evolution and (ii) efficient mapping process development for the real value outcomes of meta-heuristics to the binary domain which carried the maximum use of the real-valued explored solution.

3.1. Binary Mapping of Continuous Meta-Heuristics

In this work, thinning needed final solution appears in the binary domain; hence the applied approach to obtain the solution passed through three different phases. In the first phase, the real value solution is explored through a continuous meta-heuristic followed by transformation within the limited range in the real domain through a continuous transfer function and binarization by defining an inequality-based rule. Generally, two different forms of range limiting real-valued transfer function have been used :(i) S-shape characteristics developed by the sigmoid function as given Eq.7 and (ii)V-shape characteristics developed by Gaussian Error function as given by Eq.8. The graphical appearance of both transfer function have shown in Figure 2.

$$T(x) = \frac{1}{1+e^{-x}} \quad (7)$$

$$T(x) = \left|erf\left(\frac{\sqrt{\pi}}{2}x\right)\right| = \left|\frac{\sqrt{2}}{\pi}\int_0^{\frac{\sqrt{\pi}}{2}x} e^{-t^2}dt\right| \quad (8)$$

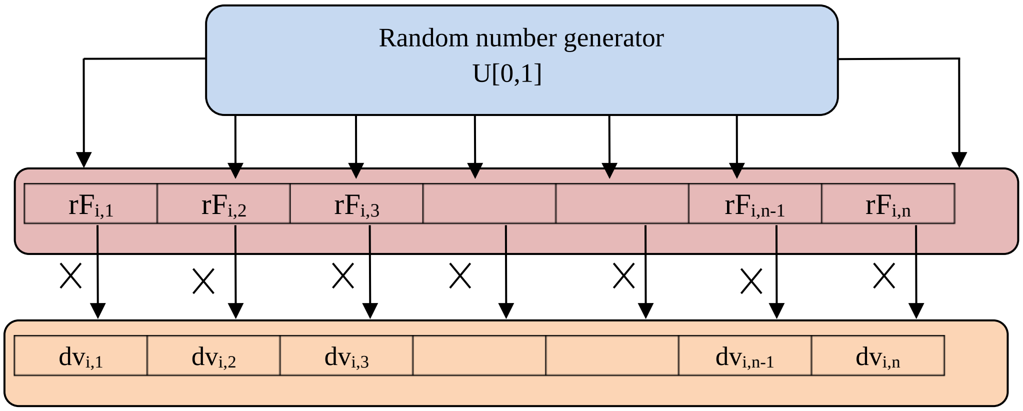

Fig. 3 Dynamic mutation factor strategy in rDE

Table 1. Applied different algorithms and their characteristics

Algorithm	Meta-Heuristic	Transfer Function	Binarization Rule
rsDE	SDE	Rounding to discrete integer	Push to the binary boundary
stSDE	SDE	Sigmoid	Threshold
spSDE	SDE	Sigmoid	Probabilistic
vpSDE	SDE	Gaussian error function	Probabilistic
strDE	rDE	Sigmoid	Threshold
rrDE	rDE	Rounding to discrete integer	Push to binary boundary

Table 2. Desired specification of the radiation pattern

Array Antenna	NAE	PSSL (dB)	FNBW(^{0})
Linear	100	-20	4.5

Table 3. Mean performances over 20 independent trials

Performance Parameter	StSDE		spSDE		rrDE	
	[F=0.5;C$_r$=0.9]	[F=0.8;C$_r$=0.5]	[F=0.5;C$_r$=0.9]	[F=0.8;C$_r$=0.5]	[C$_r$=0.9]	[C$_r$ = 0.5]
Obj.Fun	916.95	40.626	2317	1238.1	899.79	37.8
NAE	41.55	39.95	38.45	40.15	39.1	37.8
PSSL(dB)	-19.128	**-20.131**	-17.721	**-18.802**	-19.153	**-20.16**
H	0.46052	0.50416	0.4615	0.46881	0.49071	0.53391
HPBW	1.1693	1.1922	1.175	1.1864	1.2036	1.2896
FNBW	2.6589	2.8709	2.7334	2.7105	2.785	3.0772
Thinning(%)	16.9	20.1	23.1	19.7	21.8	24.4
NGC	25.6	58.8	51.25	70.4	39.55	81.95

Two different possibilities to define the inequality rule for binarization have been considered in this work: either based on direct comparing against a predefined threshold, as given by Eq.9, or under a probabilistic environment, as given by Eq.10.

$$x_{j,bin} = \begin{cases} 1 & if\ \ T(x_j) > Thr \\ 0 & otherwise \end{cases} \quad (9)$$

$$x_{j,bin} = \begin{cases} 1 & if\ \ rand(U[0,1]) < T(x_j) \\ 0 & otherwise \end{cases} \quad (10)$$

It is possible that without applying a transformation function, the outcomes of the continuous meta-heuristic can be converted into the binary form by following two steps: discretization followed by support to the nearest binary limit, as shown in Eq.11 and Eq.12.

$$x_{j,dis} = nearest\ integer\ rounding\ (x_j) \quad (11)$$

$$x_{j,bin} = \begin{cases} 1 & if\ \ x_{j,dis} > 0.5 \\ 0 & otherwise \end{cases} \quad (12)$$

3.2. Dynamic Differential Evolution (rDE)

To solve problems involving global optimization, differential evolution (DE) [11] is now regarded as one of the strongest entities within the evolutionary computation.

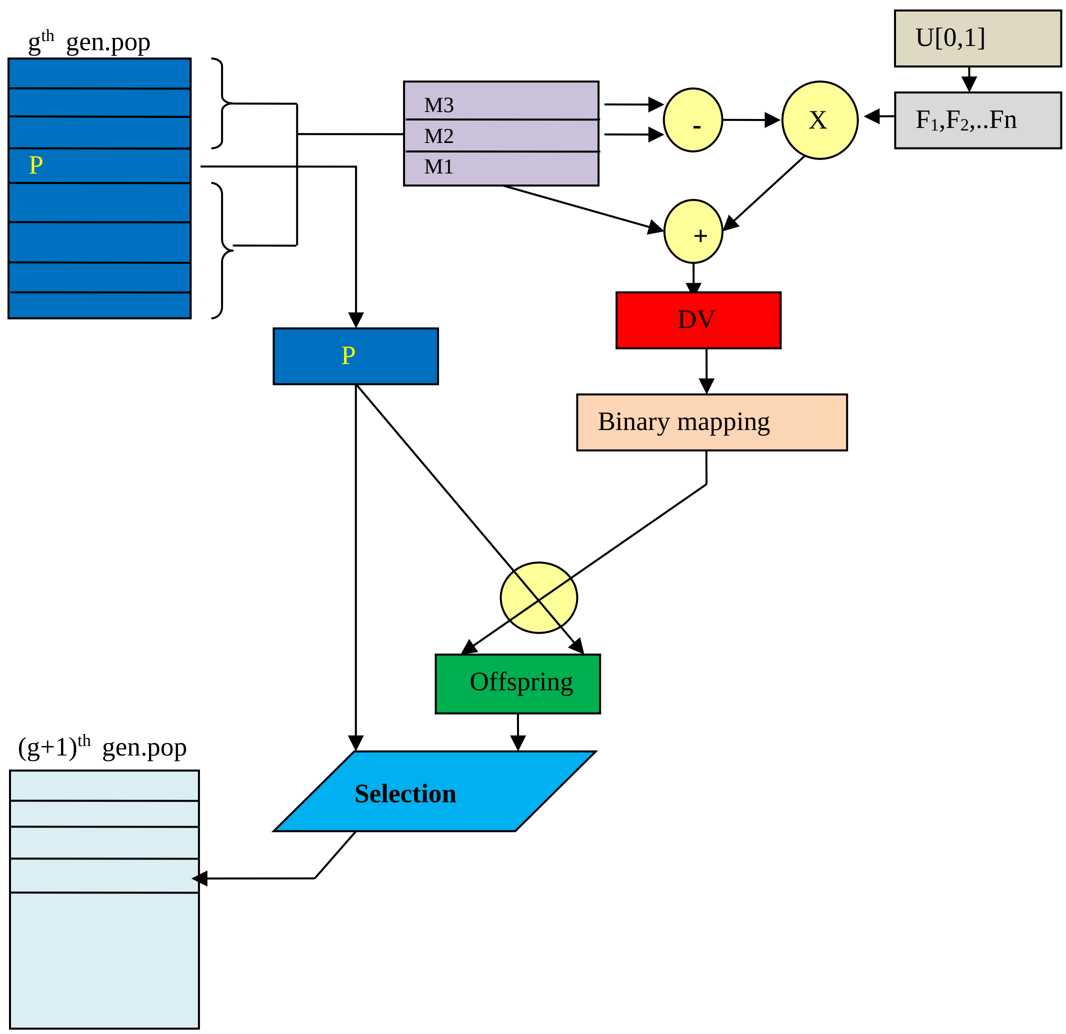

Fig. 4 The functional block diagram of rrDE

The population of the DE algorithm contains NP individuals in the standard form of DE (SDE), and each has a D-dimensional vector as per the D dimensions present in the problem. DE uses mutations to create a donor vector of dimension D over the course of one generation for each vector. The donor vector can be defined using a number of different methods. In this study, a method known as DE/rand/1, as specified in Eq. 13, has been used. The trial vector has been developed using the crossover operator in a probabilistic environment, as shown in Eq. 14. The probability of generating trial vector parameters from the mutant vector is shown by the crossover control parameter (CR), which has a range of [0, 1]. An integer in the range [1, NP] called index jrand is chosen randomly. Following that, a greedy selection operation chooses vectors for the following generation in accordance with Eq. 15 between the target and corresponding trial vectors.

$$V_i^{(G)} = X_{r1}^{(G)} + F * \left(X_{r2}^{(G)} - X_{r3}^{(G)}\right) \quad (13)$$

$$u_{ij}^{(G)} = \begin{cases} v_{ij}^{(G)} & if \;\; rand(0,1) \le CR \;\; or \; j = j_{rand} \\ x_{ij}^{(G)} & otherwise \end{cases} \quad (14)$$

$$x_{ij}^{(G)} = \begin{cases} u_i^{(G)} & if \;\; f\left(u_i^{(G)}\right) \le f\left(x_i^{(G)}\right) \\ x_i^{(G)} & othewise \end{cases} \quad (15)$$

The problem with SDE is to assign a predefined fixed value of mutation factor and crossover rate. It is well known that the value of 'F' derives from the quality of success and convergence rate. In this work, a dynamic mutation factor has been applied instead of the same fixed value of 'F' in all iterations, for all members and in all dimensions. Through the uniform distribution in the range of [0 1], a distinct random number is generated for each dimension. The whole process has shown in Figure 3, where for n dimensional problem, in the process of generating the mutation vector for the i^{th} member, each component of the differential vector $dv_{i,j}$ multiplied with the distinct random number $rF_{i,j}$.

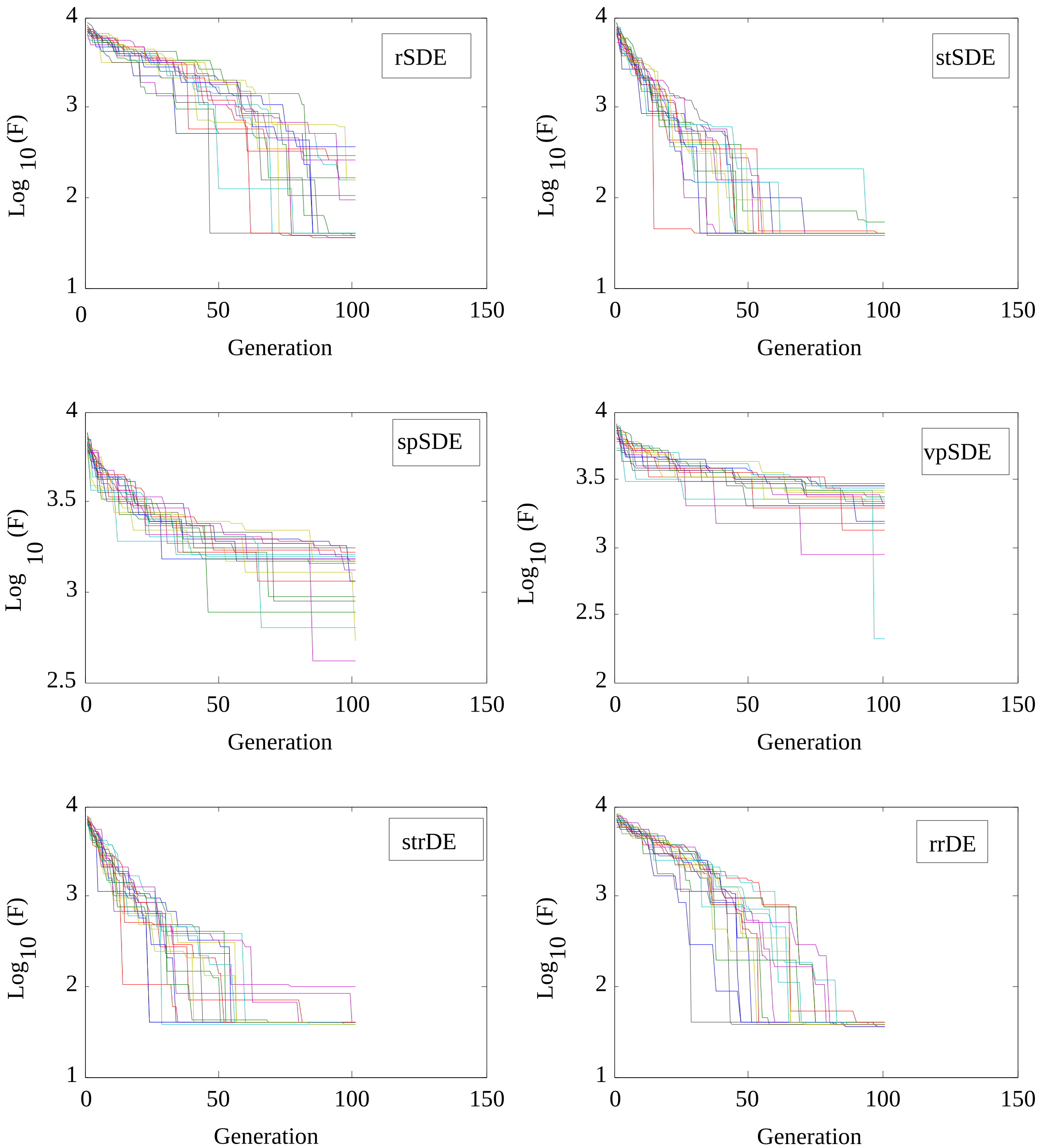

Fig. 5 Convergence characteristics by different algorithms for thinning linear array

The available diversity in the random number provided the diversity in the mutation vector and helped to explore a better solution. Because random number-based variation exists in this process, hence the DE which involves this process has been said as $rrDE$ in this paper.

In this paper, SDE and rDE have been explored with several possibilities of binary mapping, as discussed earlier. As a result, six different approaches have been applied to obtain the thinning for linear, as shown in Table 1. The functional block diagram of rrDE has shown in Figure 4.

4. Experimental Result

Simulation experiments have been given over thinning of the linear array antenna. The desired objectives' performance parameters are shown in Table 2. For the simulation purpose, fixed spacing of λ/2 between the elements has been assumed. The population size is considered 20, and the allowed generation numbers were 100. There were 20 independent trials have been considered for all considered algorithms to extract the statistical performances, and a comparison has been made over that.

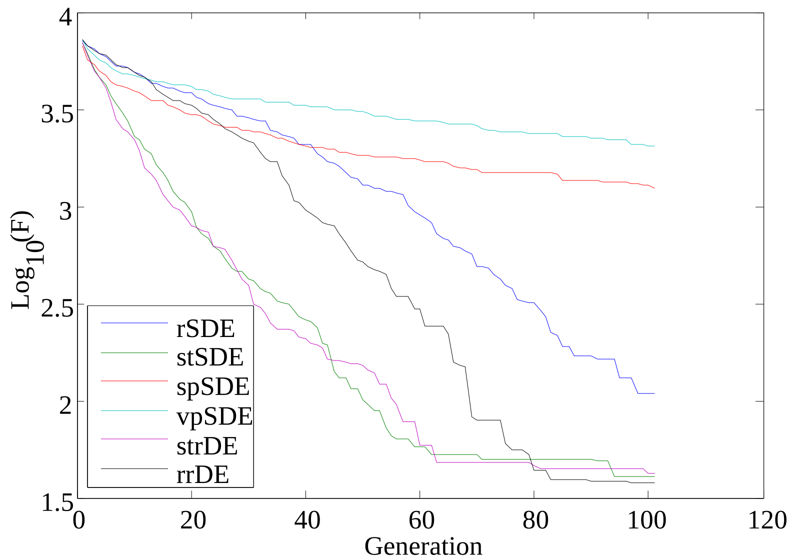

Fig. 6 Mean convergence comparison for thinning linear array

Table 4. Performance by rSDE over 20 independent trials for thinning linear array

Trial	Obj.Fun	NAE	PSSL(dB)	η	HPBW	FNBW	Thinning (%)	NGC
1	39	39	-20.652	0.52955	1.2838	2.8881	22	85
2	105.45	40	-19.935	0.49836	1.1693	2.8881	20	76
3	157.83	39	-19.881	0.50977	1.2838	3.0027	22	95
4	157.37	40	-19.883	0.49707	1.1693	2.7735	20	95
5	254.41	38	-19.784	0.52062	1.2838	3.0027	24	81
6	39	39	-20.352	0.52183	1.2838	3.0027	22	77
7	39	39	-20.147	0.51659	1.2838	3.0027	22	87
8	39	39	-20.48	0.52513	1.2838	3.0027	22	92
9	165.31	37	-19.872	0.53707	1.2838	3.1173	26	83
10	298.07	37	-19.739	0.53348	1.2838	3.1173	26	82
11	39	39	-20.011	0.5131	1.2838	2.8881	22	70
12	92.712	41	-19.948	0.48654	1.1693	2.6589	18	95
13	38	38	-20.237	0.53255	1.2838	3.1173	24	97
14	37	37	-20.015	0.54095	1.2838	3.2319	26	99
15	374.26	38	-19.664	0.51747	1.1693	2.8881	24	79
16	37	37	-20.155	0.54472	1.2838	3.1173	26	100
17	36	36	-20.175	0.56042	1.3984	3.2319	28	85
18	41	41	-20.325	0.49573	1.1693	2.7735	18	78
19	36	36	-20.064	0.55733	1.3984	3.1173	28	91
20	151.77	40	-19.888	0.49721	1.1693	2.8881	20	98

The complete simulation has been developed in the MATLAB2013a environment. The performances have been obtained in terms of objective function value as given by Eq.3, number of 'on' array elements (NAE), PSSL, Half Power beam Width (HPBW), % of thinning and point of convergence. To get a clearer idea about the involved 'on' array elements and obtained PSSL, a utilization efficiency factor η (equal to the ratio of |PSSL| and NAE) has also been obtained, and its higher value is better.

4.1. Performance of Dynamic Differential Evolution

It is known that DE performances are very responsive with respect to F and Cr values, and there are no universal values that exist for all applications. Hence, two sets of F and Cr values [0.5,0.9] and [0.8 0.5] have been examined in detail and obtained statistical performances by different algorithms, as shown in Table 3. It can be observed from Table 3 that parameter value sets of F= 0.8 and Cr=0.5 have shown better performances and hence have been considered for further experiments over thinning of the linear array.

Table 5. Performance by stSDE over 20 independent trials for thinning linear array

Trial	Obj.Fun	NAE	PSSL(dB)	η	HPBW	FNBW	Thinning(%)	NGC
1	41	41	-20.017	0.48821	1.1693	2.7735	18	71
2	54.52	41	-19.986	0.48748	1.1693	2.7735	18	94
3	40	40	-20.177	0.50443	1.1693	2.8881	20	30
4	40	40	-20.406	0.51015	1.1693	2.8881	20	47
5	39	39	-20.108	0.5156	1.1693	2.8881	22	65
6	40	40	-20.227	0.50567	1.1693	2.8881	20	39
7	38	38	-20.105	0.52907	1.2838	3.1173	24	35
8	39	39	-20.168	0.51714	1.2838	3.0027	22	82
9	41	41	-20.106	0.49039	1.1693	2.6589	18	46
10	41	41	-20.148	0.49141	1.1693	2.7735	18	45
11	40	40	-20.249	0.50623	1.1693	2.8881	20	79
12	39	39	-20.006	0.51297	1.2838	2.8881	22	38
13	40	40	-20.028	0.5007	1.1693	2.8881	20	56
14	40	40	-20.358	0.50896	1.1693	2.8881	20	49
15	40	40	-20.115	0.50287	1.1693	2.8881	20	32
16	39	39	-20.105	0.51552	1.2838	3.0027	22	67
17	41	41	-20.11	0.49049	1.1693	2.7735	18	98
18	41	41	-20.093	0.49007	1.1693	2.7735	18	94
19	39	39	-20.114	0.51574	1.1693	2.8881	22	56
20	40	40	-20.002	0.50004	1.1693	2.8881	20	53

Table 6. Performance by spSDE over 20 independent trials for thinning linear array

3 Trial	Obj.Fun	NAE	PSSL(dB)	η	HPBW	FNBW	Thinning(%)	NGC
1	1482.2	42	-18.56	0.4419	1.1693	2.6589	16	57
2	937.25	37	-19.1	0.51621	1.2838	3.0027	26	93
3	1148.3	39	-18.891	0.48438	1.1693	2.6589	22	65
4	1615.5	40	-18.425	0.46061	1.1693	2.6589	20	34
5	413.81	40	-19.626	0.49065	1.1693	2.8881	20	85
6	1489.8	41	-18.551	0.45247	1.1693	2.5444	18	53
7	1741.3	41	-18.3	0.44633	1.1693	2.5444	18	41
8	1505.9	42	-18.536	0.44134	1.1693	2.5444	16	29
9	1437.9	40	-18.602	0.46505	1.1693	2.6589	20	84
10	1462.5	40	-18.577	0.46444	1.1693	2.6589	20	99
11	1587.6	39	-18.451	0.47311	1.1693	2.7735	22	46
12	1319.7	42	-18.722	0.44577	1.1693	2.5444	16	97
13	539.78	41	-19.501	0.47564	1.1693	2.6589	18	101
14	900.29	42	-19.142	0.45576	1.1693	2.6589	16	71
15	1135.2	40	-18.905	0.47262	1.1693	2.7735	20	99
16	762.84	39	-19.276	0.49426	1.2838	3.0027	22	46
17	1651.5	39	-18.387	0.47147	1.2838	2.8881	22	96
18	625.37	41	-19.416	0.47355	1.1693	2.6589	18	66
19	1542.3	39	-18.497	0.47428	1.1693	2.6589	22	61
20	1463.3	39	-18.576	0.4763	1.1693	2.7735	22	85

As discussed in Table 1, all six different algorithms have been considered further to achieve the objectives. The convergence characteristics for all the different algorithms over 20 independent trials have shown in Figure 5.

For comparison purposes, the mean convergence characteristics have shown in Figure 6. It can observe that except rrDE has converged to the minimum value.

Table 7. Performance by vpSDE over 20 independent trials for thinning linear array

Trial	Obj.Fun	NAE	PSSL(dB)	η	HPBW	FNBW	Thinning(%)	NGC
1	2082.4	37	-17.955	0.48526	1.2838	3.0027	26	65
2	2343.6	36	-17.692	0.49145	1.2838	2.8881	28	94
3	2012.2	38	-18.026	0.47436	1.1693	2.7735	24	93
4	2768	37	-17.269	0.46673	1.1693	2.6589	26	77
5	875.3	37	-19.162	0.51788	1.2838	3.1173	26	70
6	2622.9	35	-17.412	0.49749	1.1693	2.6589	30	98
7	2853.7	37	-17.183	0.46441	1.1693	2.6589	26	74
8	2851.4	36	-17.185	0.47735	1.1693	2.7735	28	76
9	2204.5	34	-17.829	0.5244	1.3984	3.1173	32	86
10	1959.6	39	-18.079	0.46357	1.1693	2.6589	22	52
11	2229.4	35	-17.806	0.50873	1.2838	3.0027	30	26
12	1503.5	38	-18.535	0.48775	1.1693	2.6589	24	38
13	2175.2	36	-17.861	0.49613	1.2838	3.0027	28	94
14	2001.6	39	-18.037	0.4625	1.1693	2.6589	22	49
15	1568.8	42	-18.473	0.43984	1.1693	2.5444	16	90
16	2959.9	38	-17.078	0.44942	1.2838	2.7735	24	71
17	1309.1	38	-18.729	0.49287	1.2838	3.0027	24	85
18	210.23	41	-19.831	0.48368	1.1693	2.7735	18	97
19	2052.7	36	-17.983	0.49954	1.2838	3.1173	28	100
20	2533.2	40	-17.507	0.43767	1.1693	2.5444	20	64

Table 8. Performance by strDE over 20 independent trials for thinning linear array

5 Trial	Obj.Fun	NAE	PSSL(dB)	η	HPBW	FNBW	Thinning(%)	NGC
1	39	39	-20.652	0.52953	1.2838	3.0027	22	34
2	39	39	-20.037	0.51378	1.2838	2.8881	22	59
3	39	39	-20.639	0.52922	1.1693	3.0027	22	41
4	37	37	-20.086	0.54288	1.2838	3.2319	26	54
5	39	39	-20.046	0.51401	1.2838	2.8881	22	100
6	41	41	-20.623	0.50299	1.1693	2.7735	18	57
7	39	39	-20.022	0.5134	1.1693	2.8881	22	53
8	39	39	-20.263	0.51957	1.2838	3.0027	22	79
9	40	40	-20.302	0.50756	1.1693	2.8881	20	53
10	39	39	-20.087	0.51504	1.2838	2.8881	22	81
11	40	40	-20.345	0.50861	1.1693	2.7735	20	60
12	41	41	-20.4	0.49757	1.1693	2.7735	18	80
13	39	39	-20.454	0.52445	1.1693	3.0027	22	85
14	39	39	-20.144	0.51651	1.2838	2.8881	22	63
15	40	40	-20.144	0.5036	1.1693	2.8881	20	83
16	39	39	-20.262	0.51953	1.2838	3.0027	22	90
17	39	39	-20.338	0.52149	1.1693	2.8881	22	91
18	38	38	-20.561	0.54108	1.2838	3.0027	24	97
19	101.11	40	-19.939	0.49847	1.1693	2.7735	20	77
20	38	38	-20.06	0.5279	1.2838	3.1173	24	84

Table 9. Performance by rrDE over 20 independent trials for thinning linear array

Trial	Obj.Fun	NAE	PSSL(dB)	η	HPBW	FNBW	Thinning(%)	NGC
1	36	36	-20.085	0.55792	1.3984	3.2319	28	98
2	37	37	-20.028	0.54131	1.2838	3.1173	26	58
3	37	37	-20.016	0.54097	1.2838	3.1173	26	97
4	39	39	-20.056	0.51427	1.2838	2.8881	22	96
5	38	38	-20.595	0.54197	1.2838	3.1173	24	82
6	36	36	-20.18	0.56056	1.3984	3.1173	28	86
7	39	39	-20.055	0.51423	1.2838	3.0027	22	76
8	38	38	-20.069	0.52814	1.2838	3.0027	24	82
9	37	37	-20.016	0.54097	1.2838	3.1173	26	97
10	37	37	-20.278	0.54804	1.2838	3.2319	26	100
11	39	39	-20.193	0.51776	1.2838	3.0027	22	87
12	38	38	-20.29	0.53394	1.2838	3.1173	24	85
13	38	38	-20.031	0.52712	1.2838	3.0027	24	53
14	38	38	-20.122	0.52953	1.2838	3.0027	24	44
15	36	36	-20.242	0.56229	1.3984	3.2319	28	86
16	40	40	-20.198	0.50496	1.1693	2.8881	20	69
17	41	41	-20.428	0.49826	1.1693	2.7735	18	90
18	37	37	-20.2	0.54595	1.2838	3.2319	26	99
19	37	37	-20.026	0.54125	1.2838	3.2319	26	83
20	38	38	-20.093	0.52876	1.2838	3.1173	24	71

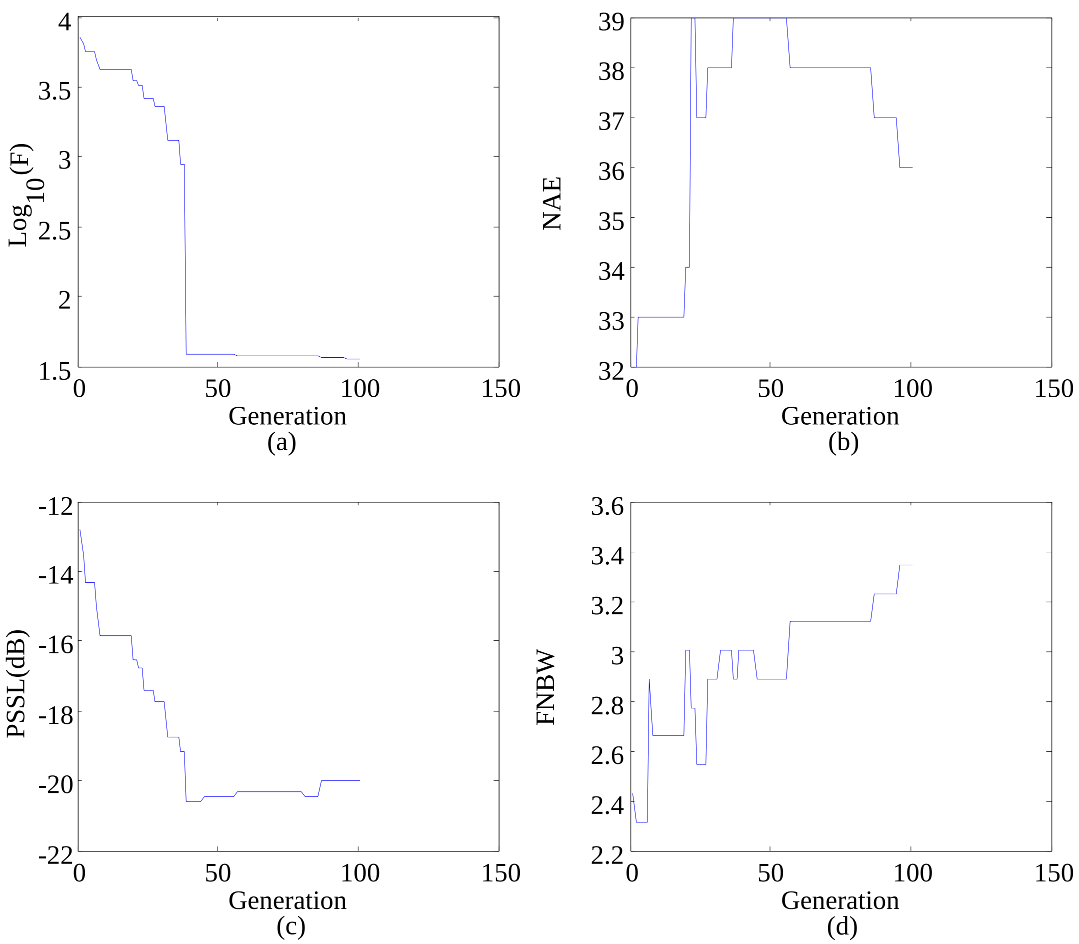

Fig. 7 Linear array thinning convergence performance in a trial for rrDE (a) objective function (b) PSSL (c) no. of array elements (NAE) (d) FNBW

Table 10. Mean (Std. dev) performance by algorithms over 20 independent trials for thinning linear array

Algorithm	Obj.Fun	NAE	PSSL(dB)	η	HPBW	FNBW	Thinning (%)	NGC
rSDE	108.86 (100.64)	38.5 (1.5044)	-20.06 (0.25558)	0.52177 (0.020722)	1.2609 (0.070541)	2.9855 (0.15453)	23 (3.0088)	87.25 (8.9022)
stSDE	40.626 (3.3795)	39.95 (0.88704)	-20.131 (0.11147)	0.50416 (0.011759)	1.1922 (0.047027)	2.8709 (0.10028)	20.1 (1.7741)	58.8 (21.513)
spSDE	1238.1 (404.92)	40.15 (1.3485)	-18.802 (0.40491)	0.46881 (0.019005)	1.1864 (0.04198)	2.7105 (0.14145)	19.7 (2.697)	70.4 (23.809)
vpSDE	2055.9 (696.13)	37.45 (2.0384)	-17.982 (0.69706)	0.48105 (0.023983)	1.2266 (0.069554)	2.8194 (0.19461)	25.1 (4.0769)	74.95 (20.992)
strSDE	42.256 (13.885)	39.2 (0.95145)	-20.27 (0.22613)	0.51736 (0.012677)	1.2266 (0.058784)	2.9282 (0.11917)	21.6 (1.9029)	71.05 (18.917)
rrDE	37.8 (1.3219)	37.8 (1.3219)	-20.16 (0.15184)	0.53391 (0.017739)	1.2896 (0.05849)	3.0772 (0.13026)	24.4 (2.6438)	81.95 (15.949)

Table 11. Thinned array elements status for thinning linear array by different algorithms

Method	Array elements conditions: 'On:1' / 'Off: 0'
rSDE	11111111111111100000000000000000000000000000000000
stSDE	11111111111111100000000000000000000000000000000000
spSDE	11111111111111100000000000000000000000000000000000
vpSDE	11111110111111100000000000000000000000000000000000
strSDE	11111111111111100000000000000000000000000000000000
rrSDE	11111111111111100000000000000000000000000000000000

Table 12. Comparative performances of rrDEagainst all array elements and PSO variant

Algorithm	NAE	PSSL(dB)	η	HPBW	FNBW	Thinning(%)
AEA	50	-13.275	0.2655	1.0547	2.3152	0
CBPSO[ ]	38	-17.077	0.4494	1.1693	2.6589	24
rrDE	36	-20.242	0.56229	1.3984	3.2319	28

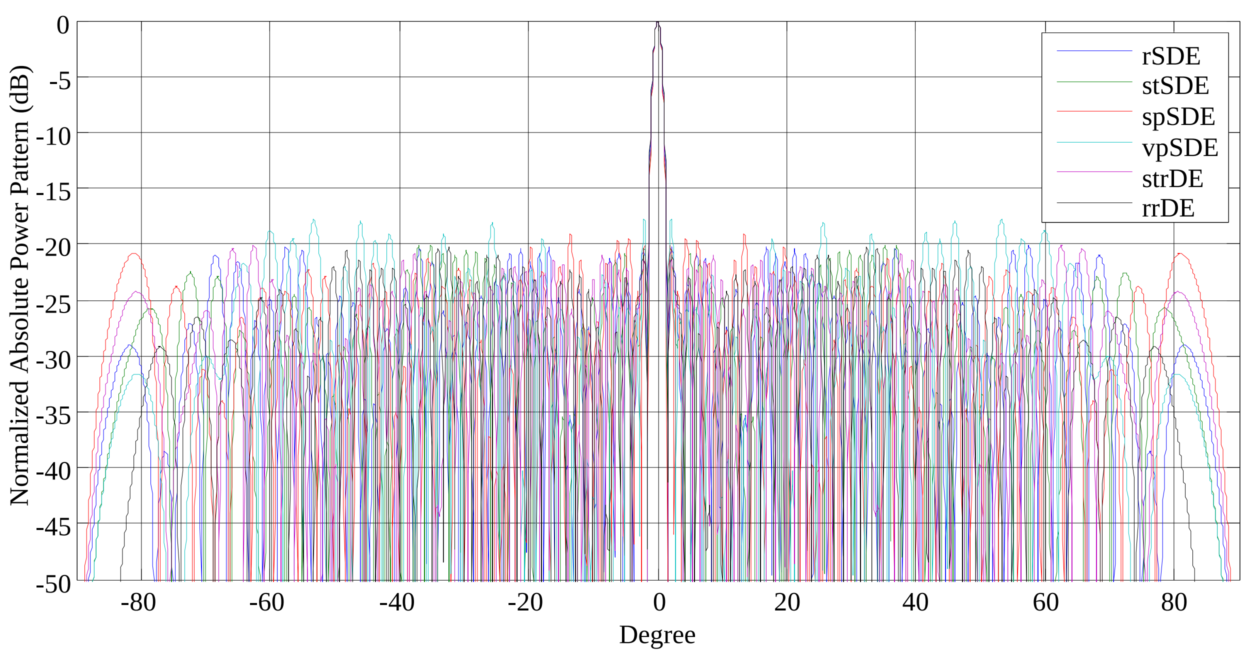

Fig. 8 Radiation pattern formed by best solution of different algorithms for linear array

Table 13. Thinned array elements status for linear array by different algorithms

Algorithm	Array elements conditions: 'On:1' / 'Off: 0'
AEA	11111111111111100000000000000000000000000000000000
CBPSO	11111111111011100000000000000000000000000000000000
rrDE	11111111111111100000000000000000000000000000000000

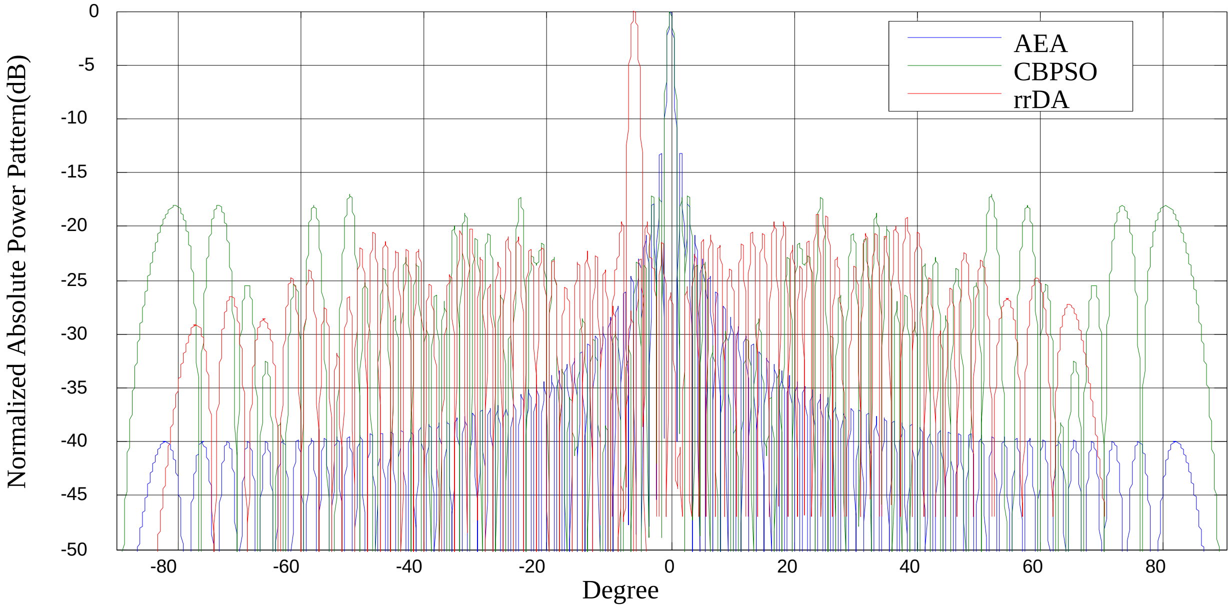

Fig. 9 Radiation pattern formed by best solution of different algorithms for linear array

The convergence rate for stSDE and strDE was faster, and the final convergence point was comparable. The performance of transformation under the probabilistic environment in the case of spSDE and vpSDE was unsatisfactory, and there were several trials for which a feasible solution could not achieve.

The obtained performances under each trial for individual algorithm have shown in Table 4 to Table 9. The statistical comparison is shown in Table 10, which clearly shows that rrDE has delivered the best performances against all other variants.

In the Table 11, the obtained best-thinned solution from each algorithm has shown. To understand the internal development of solution development in the case of rrDE, the convergence characteristics of different parameters in a test have shown in Figure 7.

In contrast, the radiation patterns corresponding to the best solution from each algorithm have shown in Figure 8.The performances of rrDE have been compared against all array elements antenna and Competitive Binary PSO (CBPSO). The AEA has shown a -13.275 dB SLL value, while CBPSO has delivered -17.0dB with 24% thinning efficiency, while rrDE has given -20.2dB SLL VALUE with 28% thinning efficiency.

The obtained best value by CBPSO has also shown in Table 11. In contrast, obtained radiation patterns have been presented in Figure 9. From the radiation pattern, the need and utility of thinning can be understood very easily.

4.2. Comparative Study of rrDE with PSO Variant

The comparative performances of rrDE against all array elements and PSO variant is shown in Table 12. The thinned array elements status for linear array by different algorithms is also shown in Table 13.

5. Conclusion

There is always interest in reducing the SLL value of radiation pattern, and in this regard solution approach to use the thinned array is always an optimum choice. This work has shown that the capability of DE to evolve a better solution has increased greatly with the dynamic mutation factor strategy.

The proposed strategy has also given the freedom from tuning the burden of the optimal value of the mutation factor. With the experimental outcomes, mapping the continuous domain to the binary domain through the transformation function has given the inferior solution, mostly because of the change in the landscape itself. The proposed solution provides the mapping over the same landscape and causes of better and faster solution. The linear array antenna geometry thinning has been examined in detail, and the proposed solution has delivered a better solution against PSO.

Reference

[1] Keen-Keong Yan, and Yilong Lu, “Sidelobe Reduction in Array-Pattern Synthesis Using Genetic Algorithm,” *IEEE Transactions on Antennas and Propagation,* vol. 45, no. 7, pp. 1117–1122, 1997. [CrossRef]

[2] Mohab Abd-Alhameed Mangoud, and H. M. Elragal, “Antenna Array Pattern Synthesis and Wide Null Control Using Enhanced Particle Swarm Optimization,” *Progress in Electromagnetics Research B*, vol. 17, pp. 1–14, 2009. [CrossRef]

[3] Narendra Nath Pathak, Banani Basu, and Gautam Kumar Mahanti, “Combination of Inverse Fast Fourier Transform and Modified Particle Swarm Optimization for Synthesis of Thinned Mutually Coupled Linear Array of Parallel Half-Wave Length Dipoles Antennas,” *Progress in Electromagnetics Research*, vol. 16, pp. 105–115, 2011. [CrossRef]

[4] Gourab Ghosh Roy et al., “Design of Non-Uniform Circular Antenna Arrays Using a Modified Invasive Weed Optimization Algorithm,” *IEEE Transactions on Antennas and Propagation*, vol. 59, no. 1, pp. 110–118, 2011. [CrossRef]

[5] Marco A. Panduro et al., “A Comparison of Genetic Algorithms, Particle Swarm Optimization and the Differential Evolution Method for the Design of Scanable Circular Antenna Arrays,” *Progress in Electromagnetics Research B*, vol. 13, no. 13, pp. 171–186, 2009. [CrossRef]

[6] Randy L. Haupt, “Thinned Concentric Ring Array,” *Proceedings of IEEE Antennas Propagation International Symposium,* San Diego, CA, pp. 1–4, 2008. [CrossRef]

[7] N. Pathak, P. Nanda, and G. K. Mahanti, “Synthesis of Thinned Multiple Concentric Circular Ring Array Antennas Using Particle Swarm Optimization,” *Journal of Infrared, Millimeter and Terahertz Waves,* vol. 30, no. 7, pp. 709–716, 2009. [CrossRef]

[8] Priyanka Pateriya, Rakesh Singhai, and Piyush Shukla, "Systematic View of STC for the Communication Systems," *SSRG International Journal of Electronics and Communication Engineering,* vol. 8, no. 11, pp. 6-14, 2021. [CrossRef]

[9] R. L. Haupt, "Interleaving Thinned Sum and Difference Linear Arrays," *2006 IEEE Antennas and Propagation Society International Symposium, Albuquerque*, NM, pp. 4773-4776, 2006. [CrossRef]

[10] Yanhui Liu, Zaiping Nie, and Qing Huo Liu, "Reducing the Number of Elements in a Linear Antenna Array by the Matrix Pencil Method," *IEEE Transactions on Antennas and Propagation,* vol. 56, no. 9, pp. 2955-2962, 2008. [CrossRef]

[11] Manoj Kumar Singh, "Discovery of Redundant Free Maximum Disjoint Set-K-Covers for WSN Life Enhancement with Evolutionary Ensemble Architecture," *Evolutionary Intelligence*, pp. 611-630, 2020. [CrossRef]

[12] Dan Busuioc, and Safieddin Safavi-Naeini, "Low-cost Antenna Array and Phased Array Architectures — Design Concepts and Prototypes," *2010 IEEE International Symposium on Phased Array Systems and Technology,* Waltham, MA, pp. 965-968, 2010. [CrossRef]

[13] A. H. Hussein et al., "Optimum Design of Linear Antenna Arrays Using a Hybrid MoM/GA Algorithm," *IEEE Antennas and Wireless Propagation Letters,* vol. 10, pp. 1232-1235, 2011. [CrossRef]

[14] B. Basua, and G.K. Mahanti, “Thinning of Concentric Two-Ring Circular Array Antenna Using Fire Fly Algorithm,” *Scientia Iranica D,* vol. 19, no. 6, pp. 1802-1809, 2012. [CrossRef]

[15] Chung-Yong Chan, and Paul M. Goggans, "Multiobjective Design of Linear Antenna Arrays Using Bayesian Inference Framework," *IEEE Transactions on Antennas and Propagation*, vol. 62, no. 11, pp. 5524-5530, 2014. [CrossRef]

[16] Smita Banerjee, and Ved Vyas Dwivedi, "Linear Antenna Array Synthesis to Reduce the Interference in the Side Lobe Using Continuous Genetic Algorithm," *2015 Fifth International Conference on Advances in Computing and Communications (ICACC),* Kochi, pp. 291-296, 2015. [CrossRef]

[17] Gui Chao Huang et al., "Antenna Array Design and System for Directional Networking," *IEEE Antennas and Wireless Propagation Letters*, vol. 14, pp. 1141-1144, 2015. [CrossRef]

[18] Shravan Kumar Namdeo, and Dr. Pramendra Tilanthe, "Performance Analysis of Smart Antenna using Particle Swarm Optimization Algorithm," *SSRG International Journal of Electronics and Communication Engineering*, vol. 2, no. 6, pp. 17-20, 2015. [CrossRef]

[19] Florin Enache et al., "Multi-Criteria Optimization of Non-Uniform Linear Antenna Array Using Genetic Algorithms," *2016 International Conference on Communications*, Bucharest, pp. 121-124, 2016. [CrossRef]

[20] Surendra Kumar Bairwa, Pawan Kumar, and Arpit Kumar Baranwal, "Enhancement of Radiation Pattern for Linear Antenna Array using Flower Pollination Algorithm," *2016 International Conference on Electrical Power and Energy Systems*, Bhopal, pp. 1-4, 2016. [CrossRef]

[21] Geng Sun et al., "Thinning of Concentric Circular Antenna Arrays Using Improved Discrete Cuckoo Search Algorithm," *2017 IEEE Wireless Communications and Networking Conference (WCNC)*, San Francisco, CA, pp. 1-6, 2017. [CrossRef]

[22] Abdelmadjid Recioui, "Thinning of Concentric Circular Arrays Using Galaxy Based Search Algorithm," *2017 5th International Conference on Electrical Engineering - Boumerdes (ICEE-B)*, Boumerdes, pp. 1-5, 2017. [CrossRef]

[23] Ali Najim Abdullah, and Laith Ali Abdul-Rahaim, "Enhancing the Performance of Localization System for Radio Frequency Transmitters Based on DOA and Triangulation algorithms," *International Journal of Engineering Trends and Technology*, vol. 69, no. 8, pp. 26-35, 2021. [CrossRef]

[24] Diego Caratelli et al., "Deterministic Constrained Synthesis Technique for Conformal Aperiodic Linear Antenna Arrays-Part I: Theory," *IEEE Transactions on Antennas and Propagation*, vol. 67, no. 9, pp. 5951-5961, 2019. [CrossRef]

[25] Geng Sun et al., "Radiation Beam Pattern Synthesis of Concentric Circular Antenna Arrays Using Hybrid Approach Based on Cuckoo Search," *IEEE Transactions on Antennas and Propagation*, vol. 66, no. 9, pp. 4563-4576, 2018. [CrossRef]

[26] Krishanu Kundu, and Narendra Nath Pathak, “Circular Antenna Array Optimization Using Flower Pollination Algorithm,” *Advances in Computer, Communication and Control. Lecture Notes in Networks and Systems, Springer*, Singapore, vol. 41, pp. 407-414, 2019. [CrossRef]

[27] Amiya Kumar Mondal, and Prerna Saxena, "Thinning of Concentric Circular Antenna Array Using Binary Salp Swarm Algorithm," *2019 IEEE Conference on Information and Communication Technology*, Allahabad, India, pp. 1-4, 2019. [CrossRef]

[28] Shruti. R. Danve, Manoj S. Nagmode, and Shankar B. Deosarkar, "Transmit Antenna Selection in Massive MIMO: An Energy-Efficient Approach," *International Journal of Engineering Trends and Technology*, vol. 70, no. 12, pp. 170-178, 2022. [CrossRef]

[29] Avishek Das, D. Mandal, and R. Kar, “An Efficient Concentric Circular Antenna Array Synthesis Considering the Mutual Coupling,” *Proceedings of the 2nd International Conference on Communication, Devices and Computing, Lecture Notes in Electrical Engineering, Springer*, Singapore, vol. 602, pp. 45-53, 2020. [CrossRef]

[30] Tingting Zheng et al., "IWORMLF: Improved Invasive Weed Optimization with Random Mutation and Lévy Flight for Beam Pattern Optimizations of Linear and Circular Antenna Arrays," *IEEE Access*, vol. 8, pp. 19460-19478, 2020. [CrossRef]

[31] Dr. Thota Vidhyavathi, "Amplitude and Phase Synthesis of Linear Array for Sector Beams using Modified Harmony Search Differential Evolution Algorithm," *SSRG International Journal of Electronics and Communication Engineering*, vol. 3, no. 8, pp. 20-27, 2016. [CrossRef]

[32] R. L. Haupt, "Interleaved Thinned Linear Arrays," *IEEE Transactions on Antennas and Propagation*, vol. 53, no. 9, pp. 2858-2864, 2005. [CrossRef]

[33] Nechaev Yuri, and Peshkov Ilia, "Probability of False Peaks Occurring via Circular and Concentric Antenna Arrays DOA Estimation," *2016 39th International Conference on Telecommunications and Signal Processing (TSP)*, Vienna, pp. 178-181, 2016. [CrossRef]

[34] Xiao Luo, Yong-Jian Yang, and Qian-Yu Zhou, "A Firefly-Cuckoo Search Algorithm for Optimizing the Beam Patterns of the Random Antenna Arrays," *2018 4th Annual International Conference on Network and Information Systems for Computers (ICNISC)*, Wuhan, China, pp. 84-88, 2018. [CrossRef]

[35] Gebrehiwet Gebrekrstos Lema, Dawit Hadush Hailu, and Tekle Brhane Wuneh, “SLL Attenuation-Based Thinned Antenna Design for Next-Generation Communications,” *EURASIP Journal on Wireless Communications and Networking*, vol. 225, 2019. [CrossRef]